Antagonist Inhibition Control in Redundant Tendon-Driven Structures Based on Human Reciprocal Innervation for Wide Range Limb Motion of Musculoskeletal Humanoids

Kento Kawaharazuka, Masaya Kawamura, Shogo Makino, Yuki Asano, Kei Okada, and Masayuki Inaba

Abstract—The body structure of an anatomically correct tendon-driven musculoskeletal humanoid is complex, and the difference between its geometric model and the actual robot is very large because expressing the complex routes of tendon wires in a geometric model is very difficult. If we move a tendon-driven musculoskeletal humanoid by the tendon wire lengths of the geometric model, unintended muscle tension and slack will emerge. In some cases, this can lead to the wreckage of the actual robot. To solve this problem, we focused on reciprocal innervation in the human nervous system, and then implemented antagonist inhibition control (AIC)-based on the reflex. This control makes it possible to avoid unnecessary internal muscle tension and slack of tendon wires caused by model error, and to perform wide range motion safely for a long time. To verify its effectiveness, we applied AIC to the upper limb of the tendon-driven musculoskeletal humanoid, Kengoro, and succeeded in dangling for 14 min and doing pull-ups.

Index Terms—Biomimetics, humanoid robots, tendon/wire mechanism.

I. INTRODUCTION

IN RECENT years, the development of tendon-driven musculoskeletal humanoids is very vigorous [1], [2]. So far, many topics such as its joint structure, arrangement of muscles, design approach and so on have been discussed. However, its joint structure and drive system are very complex because they are based on the human body. This becomes a big problem when moving the actual robot. For an ordinary robot, we make a geometric model and test the motion in a simulation environment. After that, we verify that the actual robot moves correctly. However, the difference between the geometric model and the actual robot in a tendon-driven musculoskeletal humanoid is very large because it is impossible to fully express the complex routes of tendon wires in a geometric model.
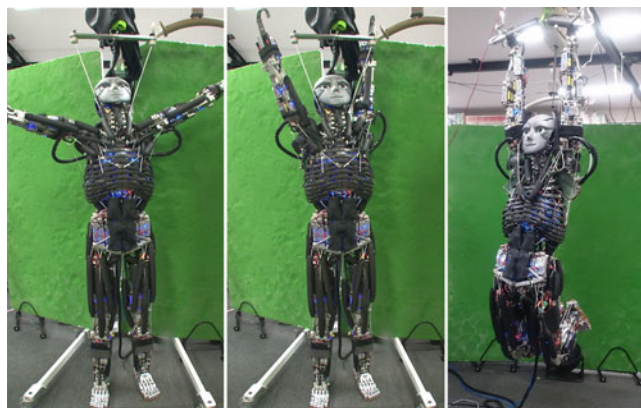
Fig. 1. Example of wide range upper limb motion.

To solve this problem, we can make a more complex and detailed geometric model, or implement a new control system which can absorb model error. There are some studies about modeling detailed tendon-driven musculoskeletal humanoids, but they are difficult to introduce, computationally complex, and unable to solve model error as much as an ordinary robot. Also, there are only a few studies moving the actual robot using the detailed model, much less doing wide range motion such as raising the arms using the scapula and shoulder (Fig. 1), in which model error is fatal.

There are also some studies about the control of tendon-driven musculoskeletal humanoids. They include the simple control of movements by the wire length of the geometric model, muscle stiffness control [3], position and force control with rectifiers [4], puller-follower control [5], and joint-space control [6], [7]. However, if we attempt to move the actual robot in a wide range using these controls, large internal muscle tension emerges due to model error, or the robot cannot move to the desired position because it is assumed that the geometric model is correct. Therefore, there are few experiments using not the geometric model but the actual tendon-driven musculoskeletal humanoid, much less one that achieves wide range motion. Also, experiments of the actual robot are almost always done using the uniaxial elbow joint with an encoder, and experiments using the ball joints in the shoulder or the complex scapula are done by using motion capture, which needs large-scale setup. This is a big problem,

and we believe that it interferes with the popularization of the tendon-driven musculoskeletal humanoid, which is the ultimate humanoid based on the human body.

To move the tendon-driven musculoskeletal humanoid smoothly without accumulating internal muscle tension, we focused on the human nervous system. There are some reflexes in the human nervous system such as the stretch reflex, the tendon reflex, and reciprocal innervation, and among them, humans are able to move their bodies smoothly by reciprocal innervation, which inhibits antagonist muscles. We hypothesized that wide range motion could be achieved by applying this reciprocal innervation to the tendon-driven musculoskeletal humanoid. Although the control of pneumatic artificial muscles (PAMs) is similar to the control in this study in the sense that they both inhibit antagonist muscles, they are actually completely different. The control of PAMs controls muscles having simple antagonistic relationships by pressure, but the control in this study does position control according to the complex relationship of agonist and antagonist muscles as the antagonistic states correspond to the limb posture. There is the related work of muscle load sharing among agonist muscles [8], but what we want to focus on is the study between agonist muscles and antagonist muscles. Additionally, we aimed to develop a system in which an encoder or motion capture is unnecessary by using the estimation method of the joint angle [9]. This method cannot estimate the joint angle of the complex shoulder or scapula very accurately, but the error is tolerated by using the joint angle only for the decision of whether a muscle is an agonist or antagonist muscle.

In this study, we show that the tendon-driven musculoskeletal humanoid, which could not move in a wide range owing to large model error, can achieve wide range motion without accumulating internal muscle tension using the simple antagonist inhibition control (AIC) system based on reciprocal innervation. Then, we discuss the difference between this study and other control systems.

II. SYSTEM OF THE TENDON-DRIVEN MUSCULOSKELETAL HUMANOID, KENGORO

A. Tendon-Driven System of Kengoro

The robot we use for this study is the tendon-driven musculoskeletal humanoid, "Kengoro" [2]. This robot is modeled after the human body, including its joint structure, body proportion, weight ratio, and joint performance, and is used as the research platform for the human body simulator and full-body contact behavior. The drive system is composed of 116 sensor-driver integrated muscle modules [10] and duplicates the major muscles of a human. As Fig. 2 indicates, the muscle module has a brushless DC motor, a gear head, a pulley that winds wire, a Dyneema that acts as muscle wire, a temperature sensor that monitors muscle temperature, a tension measurement unit (weight limit: about 55 [kgf]), and a motor driver that can do current control. Dyneema is a chemical fiber that is resistant to abrasion. It can be a cause of model error because it extends by muscle tension as shown in [8]. To allow flexible contact with the environment, there is a foam cover and a spring that prevents the inhibition of muscle movement around the Dyneema.
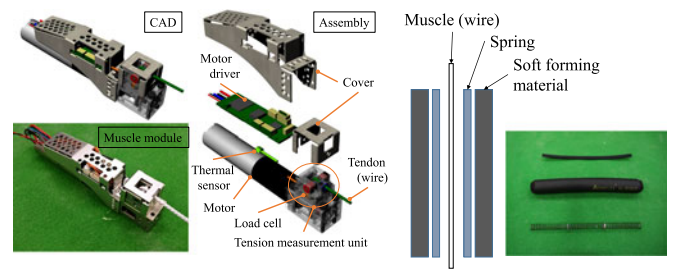

Fig. 2. Structure of Kengoro's muscle module [2], [10]. Left: sensor-driver integrated muscle module. Right: muscle wire and foam cover.
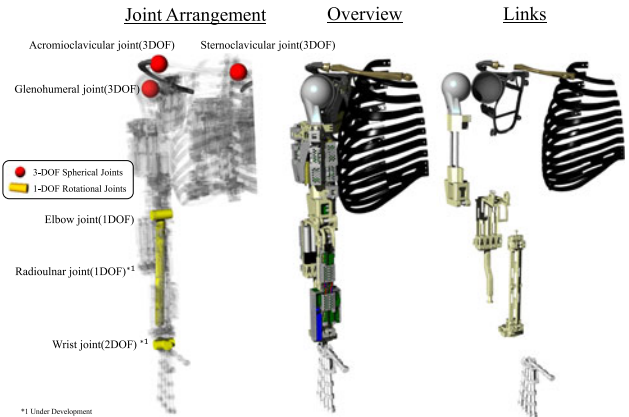

Fig. 3. Structure of Kengoro upper limb.

However, this becomes a cause of difficulty when modeling the route of muscles. As reference, the gear ratio of this muscle module is 29:1 in most cases, and the temperature starts to rise when the muscle tension is more than about 30 [kgf].

B. Structure of Kengoro Upper Limb

The human upper limb extends from the sternum to the clavicle, scapula, humerus, ulna, and radius, in order. The sternum and clavicle are connected by the sternoclavicular (SC) joint, the clavicle and scapula are connected by the acromioclavicular (AC) joint, the scapula and thorax are connected by the scapulothoracic (ST) joint, and the scapula and humerus are connected by the glenohumeral joint (GH). This structure of the human body applies to Kengoro, as shown in Fig. 3. The movement of the shoulder is composed of the GH joint, which is a ball joint that has 3 DOFs. The movement of the scapula is composed of a 3 DOFs joint (upward rotation, downward rotation, adduction, abduction, elevation, depression) because the SC and AC joints, having 6 DOFs total, are constrained by the ST joint. We cannot raise our arms with just the GH joint in the shoulder. We are able to raise our arms by the upward rotation of the scapula, along with the movement of the shoulder joint. This ratio is said to be 2:1, and that the scapula rotates upward by 60 [deg] when the abduction of the shoulder is by 120 [deg]. Therefore, simultaneous movement of the scapula and shoulder is important for wide range upper limb motion such as touching one's back and dangling.
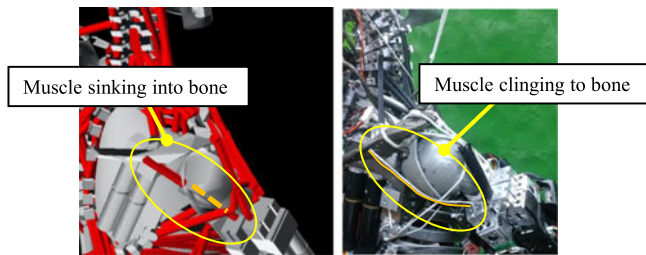
Fig. 4. Geometric model and actual robot.

C. Comparison Between Geometric Model of Kengoro and Actual Kengoro

The geometric model of the tendon-driven musculoskeletal humanoid is very complex and difficult. In the geometric model of Kengoro, we model the route of muscle wires by arranging the start point, end point, and multiple relay points. However, this method has a big problem. The problem is that we cannot model the route of the wires perfectly because, as shown in Fig. 4, the muscle of the actual robot clings around the structure, but the muscle of the geometric model sinks into the structure. At the same time, due to the complex structure, the route of muscle wires can deviate from the desired path depending on the joint angle.

III. SYSTEM OF ANTAGONIST INHIBITION CONTROL

A. Reciprocal Innervation in Humans

First, we want to consider how humans control their bodies. The principle of the human nervous system is indicated in Fig. 5. There are sensory receptors called the muscle spindle and the tendon organ in the muscle.

The muscle spindle is a spindle-shaped organ adhered parallel to the muscle fiber, and is a receptor that detects muscle length and shrinkage velocity. This creates a reflex loop called the stretch reflex, and consists of a negative feedback system based on muscle length.

The tendon organ is arranged at the edge of the muscle, and is connected to the muscle fiber in series. This creates a reflex loop called the tendon reflex, which consists of a negative feedback system based on muscle tension.

What we want to focus on in this study is reciprocal innervation in the human nervous system. Muscles can create tension only in the direction of contraction, so one or more pairs of antagonistic muscles have to exist in order for the smooth movement of the joints to occur. Of the antagonistic muscle pairs, muscles that contract in the direction of joint movement are called agonist muscles, and the others are called antagonist muscles. Therefore, to move the body smoothly, we need to stimulate α motor neurons of agonist muscles and inhibit those of antagonist muscles. In the human body, a neural circuit that stimulates motor neurons of agonist muscles and at the same time inhibits those of antagonist muscles is equipped. Such reciprocal interaction between agonist and antagonist muscles is called reciprocal innervation. This neural circuit between mus-
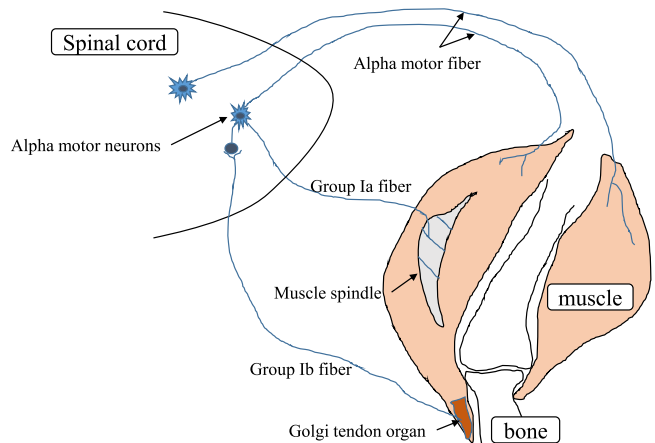

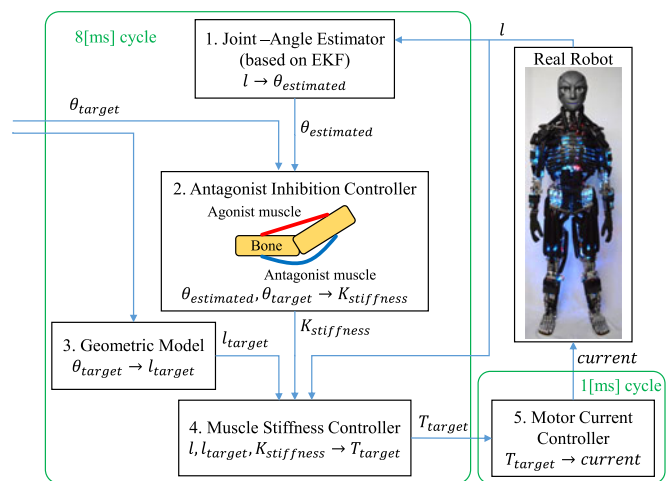Fig. 5. The principle of human reciprocal innervation.

Fig. 6. System of antagonist inhibition control.

cles is complex, and in this study, we developed antagonist inhibition control by imitating this complex reciprocal action.

B. System of Antagonist Inhibition Control

The newly implemented antagonist inhibition (AIC) system is a simple control system to change the muscle stiffness gain of muscle stiffness control (MSC) between agonist and antagonist muscles. The overview of the system is shown in Fig. 6, and each topic will be explained respectively.

1) Joint-Angle Estimator: We must estimate the joint angle from the change in muscle length because the angle of the ball joint cannot be measured by the rotary encoder, potentiometer, and so on. We use the estimation method of the joint angle proposed by Okubo, *et al.* [9]. We can estimate the joint angle of the actual robot from the change in muscle length by Extended Kalman Filter.

2) Antagonist Inhibition Controller: This is the most important part in this study. We want to inhibit muscle tension of antagonist muscles like in reciprocal innervation. Muscle jacobian $G(\boldsymbol{\theta})$ is expressed as below.

$$G(\boldsymbol{\theta}) = d\boldsymbol{l}/d\boldsymbol{\theta} \tag{1}$$

This ($l \times n$) matrix (l is the number of muscles, n is the number of joints) expresses how much the muscle contracts when the joint moves in a certain direction while the joint angle is $\boldsymbol{\theta}$. In other words, when the target joint angle is $\boldsymbol{\theta}_{target}$, and the current joint angle is $\boldsymbol{\theta}$, $G(\boldsymbol{\theta})(\boldsymbol{\theta}_{target} - \boldsymbol{\theta})$ expresses whether each muscle is an agonist muscle or an antagonist muscle when moving to that position. In this study, we change the muscle stiffness $K_{stiffness}$ depending on if the muscle is an agonist or antagonist muscle. When $K_{stiffness}$ is positive, the muscle causes tension in the direction of the target length $\boldsymbol{l}_{target}$, and when $K_{stiffness}$ is 0, the muscle tension is constant at $\boldsymbol{T}_{bias}$. These represent agonist and antagonist muscles exactly, and the AIC system decides as below regarding the i-th muscle:

$$s = G(\boldsymbol{\theta})\frac{\boldsymbol{\theta}_{target} - \boldsymbol{\theta}}{|\boldsymbol{\theta}_{target} - \boldsymbol{\theta}|}[i] \tag{2}$$

$$\boldsymbol{K}_{stiffness}[i] = k \quad \text{if} \quad s < C \tag{3}$$

$$\boldsymbol{K}_{stiffness}[i] = 0 \quad \text{if} \quad s \geqq C \tag{4}$$

where s represents moment arm in the intended direction by the normalization of ($\boldsymbol{\theta}_{target} - \boldsymbol{\theta}$), k is the constant value given to $\boldsymbol{K}_{stiffness}$ of agonist muscles, and C is the threshold value which decides the antagonistic state. To stabilize movement, we change $\boldsymbol{K}_{stiffness}$ linearly from 0 to k, and then from k to 0 in t_k[msec].

Also, we will show how to obtain the muscle jacobian. There are polyarticular muscles in the human body; for example, the pectoralis major muscle is influenced by the movement of the scapula and shoulder joints. Like the method proposed by Okubo *et al.* [9], we focus on a certain muscle, and formulate its muscle length as a polynomial of related joint angles using data from the geometric model. Then, we differentiate the polynomial to obtain the muscle jacobian.

3) Geometric Model: When we give the target joint angle to the geometric model, such as in the left picture of Fig. 4, we can find the target muscle length from the start point, the relay points, and the end point of the muscle.

4) Muscle Stiffness Controller: In MSC, the target muscle tension is decided by multiplying muscle stiffness by the difference between the target muscle length and the current muscle length.

$$\boldsymbol{T}_{target} = \boldsymbol{T}_{bias} + \max\{0, \boldsymbol{K}_{stiffness}(\boldsymbol{l} - \boldsymbol{l}_{target})\} \tag{5}$$

The $\boldsymbol{T}_{bias}$ is added in order to prevent the loosening of the muscle.

5) Motor Current Controller: This is the part that converts from the target muscle tension to the actual current that flows to the muscle motor.

IV. CHARACTERISTICS OF ANTAGONIST INHIBITION CONTROL

In this section, we will show some characteristics of AIC in order to better understand the benefits.

A. Analogy with Human Reciprocal Innervation

We mentioned above that human reciprocal innervation decides antagonistic states by the complex interaction between
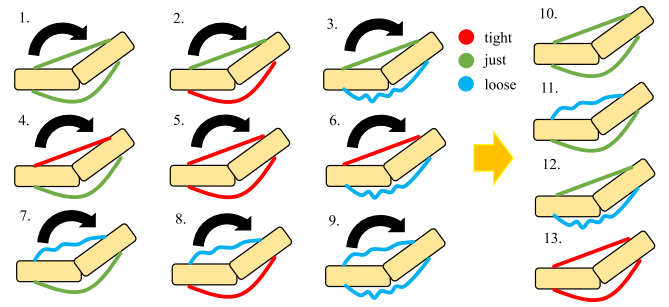

Fig. 7. Various types of antagonistic model error.

muscles. On the other hand, the operation flow of AIC is shown as below. First, in AIC, the joint angle is estimated with a complex formula using changes in muscle lengths [9]. Then, the muscle jacobian of a certain muscle is obtained as a polynomial of the involved joint angles. AIC moves based on the antagonistic states obtained by the estimated joint angle, muscle jacobian, and intended posture. This means that AIC is based on the complex interactions of the changes in muscle lengths in the time direction, and that AIC can artificially imitate the complex muscle interactions of human reciprocal innervation. Also, the value s obtained by the antagonistic states is the degree of excitation and inhibition of the $alpha$ motor neuron. AIC imitates human reciprocal innervation by regarding the excitation as the control that follows the target length, and inhibition as the control that keeps constant muscle tension.

B. Classification of Antagonistic States

There are 9 types of states in antagonistic muscles, shown as types 1–9 in Fig. 7.

There are 3 types of muscle tension states, which are just right, loose, and tight, and they result in 9 combinations of antagonistic states. When the joint moves in the direction of the arrow, the antagonistic state changes among these 9 states, and finally stops at states 10–13, which are stable. Among the final states, 10 is the best state because it has no model error and can keep adequate muscle tension. 11 and 12 are states in which the muscle length of the actual robot is consistent with that of the geometric model, but either one could become loose due to model error, and 13 is the state in which the muscle wires pull each other, resulting in high muscle tension. In these states, the most dangerous state is 13. In state 13, the larger the model error is, the more the muscles pull each other, and can lead to fatal damage to the muscles or bones. The most important benefit of AIC is that it can avoid state 13 completely because it does not assume that its geometric model is absolutely correct. In AIC, antagonist muscles do not follow the target muscle length, and keep a constant muscle tension, so state 13 always stops at state 10. AIC can also prevent the slack of muscle wires using the same principle. On the other hand, if we assume that the geometric model is correct in spite of the model error, we cannot avoid states 11, 12, and 13.

C. Comparison Between AIC and Another Simple Control

We propose another new control and discuss its differences with AIC for better understanding. In AIC, we use whether the value as stated below is positive or negative in order to decide between agonist or antagonist muscle.

$$s = G(\boldsymbol{\theta})(\boldsymbol{\theta}_{target} - \boldsymbol{\theta})[i] \qquad (6)$$

where we have removed the denominator $|\boldsymbol{\theta}_{target} - \boldsymbol{\theta}|$ for easier understanding. The value as stated above seems to equal the value shown below because $\boldsymbol{\theta}_{target} - \boldsymbol{\theta}$ is $d\boldsymbol{\theta}$, and $G(\boldsymbol{\theta})d\boldsymbol{\theta}$ is $d\boldsymbol{l}$.

$$s = (\boldsymbol{l}_{target} - \boldsymbol{l})[i] \qquad (7)$$

Thus, we can propose another control system using the value above for the decision of agonist or antagonist muscle. We will refer to the basic AIC as joint-based AIC, and the now proposed AIC as the muscle-based AIC. In joint-based AIC, when the muscles are antagonistic in the geometric model, the antagonist muscle is inhibited against the agonist muscle. This can avoid state 13 completely. On the other hand, in muscle-based AIC, muscles contract simply if they want to contract, and muscles keep constant muscle tension if they want to extend. In this case, the muscles could end up in state 13 because if the antagonist muscle contracted more than $\boldsymbol{l}_{target}$ due to model error, the antagonistic muscles pull each other. At a glance, the two controls seem to be the same, but muscle-based AIC is not practical because it cannot avoid state 13. The difference is that whereas muscle-based AIC uses the current muscle length as it is, joint-based AIC uses the estimated joint angle from the current muscle length. If we use the muscle length of the actual robot, the model error becomes large, but if we convert the actual muscle length to the joint angle of the geometric model, it is not influenced by model error because it has the idealistic conditions of the model. Additionally, we only decide between agonist or antagonist muscle in AIC, and this makes it hard for antagonistic model error to occur. For example, at the uniaxial joint shown in Fig. 7, the model error due to muscle length can of course occur, but the antagonistic state does not change between the geometric model and the actual robot.

D. Other Characteristics

First, we will focus on the constant value C used in the decision of antagonistic states. C expresses the threshold of the moment arm in the intended direction. However small the moment arm of the muscle is, when C equals 0, if s is negative, the muscle is an agonist muscle, and vice versa. This is theoretically correct, so we set C equal to 0 in this study. However, the muscle jacobian $G(\theta)$ is obtained by the geometric model, the moment arm of the muscle has model error in a certain degree, and the correct antagonistic states are not necessarily obtained by whether the moment arm is positive or negative. Although incorrect antagonistic states can emerge by model error, the muscles making incorrect antagonistic states have only small moment arm, so internal muscle tension does not accumulate. Also, if C becomes bigger in the negative direction, all of the agonist muscles which have only small moment arm in
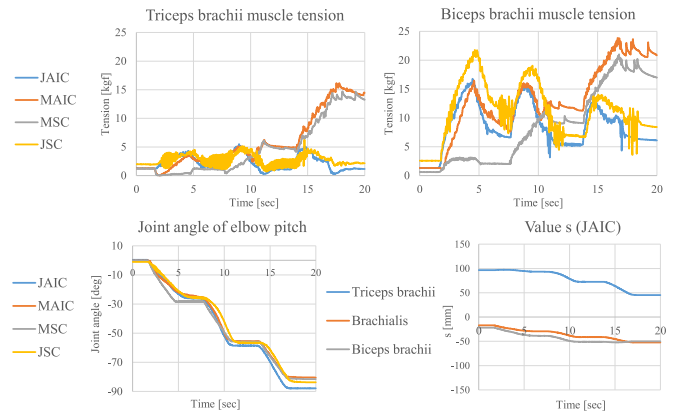

Fig. 8. Basic experiment of elbow joint. Upper graph shows comparison of muscle tensions of biceps and triceps brachii among joint-based AIC (JAIC), muscle-based AIC (MAIC), muscle stiffness control (MSC), and joint space control (JSC). Lower left graph shows joint angle of the elbow pitch, and lower right shows value s of JAIC.

the intended direction are inhibited, and the effect of antagonist inhibition becomes bigger. Thus, even if there is model error, we can make sure that incorrect antagonistic states do not emerge. Since movement in the unintended direction is permitted to a certain degree, we can see that the joint moves in the direction in which the muscle tension between agonist muscles become equal. However, at the same time, this creates unintended movement. On the other hand, if C becomes bigger in the positive direction, the effect of antagonist inhibition becomes smaller, but this does not create unintended movement because the antagonist muscles that have small moment arm in the direction of movement inhibition act as agonist muscles.

Next, we will focus on the estimated joint angle. The estimation result of a complex joint cannot be said to be very accurate. However, in AIC, agonist muscles of the actual robot follow the geometric model, and the estimated joint angle is only used for the decision of the antagonistic state. Thus, the inaccuracy of the estimated joint angle does not become a big problem because it is hard for antagonistic model error to occur.

E. Basic Experiment of Elbow Joint

Before the wide range limb motion experiment, we conducted an easy experiment of the uniaxial elbow joint. The uniaxial elbow joint of Kengoro is composed of three muscles: the triceps brachii, brachialis, and biceps brachii. We used a simple model representing the route of muscles by only the starting and end points as the geometric model of the elbow joint for easy understanding of the result. We moved the elbow joint of Kengoro up to 90 [deg] by 30 [deg] using joint-based AIC (JAIC), muscle-based AIC (MAIC), muscle stiffness control (MSC), and joint space control (JSC, [7]). We show the result in Fig. 8.

We can see similar behavior regarding internal muscle tension between MAIC and MSC. This is because the antagonistic state of MAIC finally comes to state 13 by model error as mentioned above, and agonist and antagonist muscles attract strongly together. Compared with JAIC, the joint angle trajectories of MAIC and MSC are poor at -90 [deg], but MSC
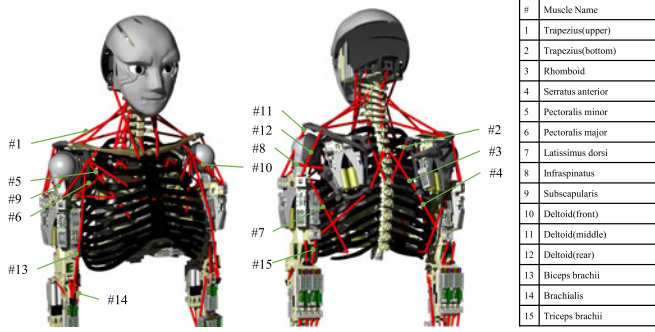
#	Muscle Name
1	Trapezius(upper)
2	Trapezius(bottom)
3	Rhomboid
4	Serratus anterior
5	Pectoralis minor
6	Pectoralis major
7	Latissimus dorsi
8	Infraspinatus
9	Subscapularis
10	Deltoid(front)
11	Deltoid(middle)
12	Deltoid(rear)
13	Biceps brachii
14	Brachialis
15	Triceps brachii

Fig. 9. Muscle arrangement of Kengoro upper limb. #1–#7 is related to motion of the scapula and #6–#15 is related to motion of the shoulder.

is stable while the movement is small because of cocontraction. JAIC and JSC also show similar behavior, but JSC causes muscles to vibrate easily and is poor at joint angle trajectory because of a torque control using only muscle jacobian. JSC is influenced strongly by the model error of muscle jacobian; for example, Kengoro can raise the complex shoulder roll joint by only 60 [deg] in response to a command of 120 [deg]. On the other hand, in JAIC, from the value s, we can see that brachialis and biceps brachii are always agonist muscles and triceps brachii is always an antagonist muscle, so large internal muscle tension is avoided. Also, even if $\boldsymbol{\theta}$ surpasses $\boldsymbol{\theta}_{target}$, the positive and negative of this value s merely becomes reversed, and large internal muscle tension can be avoided completely.

For these reasons stated in the subsections, AIC can move the actual robot without fatal damage by using a somewhat accurate geometric model of the complex tendon-driven musculoskeletal humanoid, which is difficult to model. In addition, AIC can fulfill its significance as the human simulator because it is based on the human nervous system.

V. ACHIEVEMENT OF WIDE RANGE UPPER LIMB MOTION BY ANTAGONIST INHIBITION CONTROL

We conducted experiments on wide range upper limb motion, which can be safely achieved using AIC. First, we will show the effectiveness of this control based on experiments conducted on the shoulder, and then on the scapula. Second, we conducted experiments of raising the arm using the shoulder and scapula, and checked the feasibility of this motion. For comparison, we used the basic control method, muscle stiffness control (MSC), in which $K_{stiffness}$ is constant. Finally, we conducted dangling and pull-up experiments, which become possible as a result of avoiding the internal muscle tension due to model error. In all of these experiments using AIC and MSC, T_{bias} is 2 [kgf], k is 10, C is 0, and t_k is 1000 [msec].

A. Movement Using the Shoulder by AIC

The shoulder is driven by ten muscles, #6–#15, of those in Fig. 9. The experimental motion is doing abduction as in Fig. 10, and doing adduction after that. The results of this experiment are indicated in Fig. 11. In this experiment, the maximum muscle tension decreased from 43 [kgf] to 28 [kgf] in AIC as compared to MSC. Especially, the subscapularis muscle
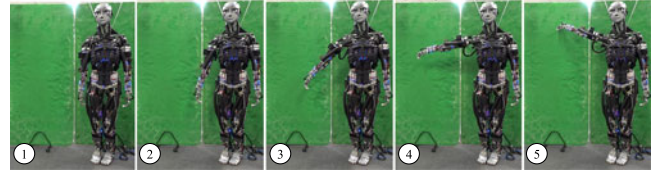

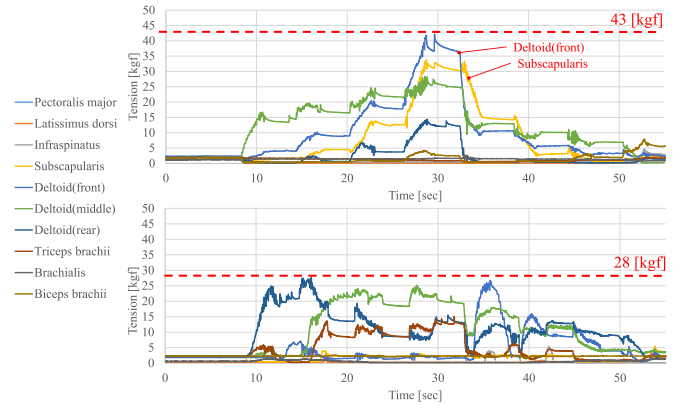Fig. 10. Experimental motion of shoulder.

Fig. 11. Result of shoulder motion experiment. Comparison of muscle tension between muscle stiffness control (upper graph) and antagonist inhibition control (lower graph).

and deltoid(front) display very high muscle tension in MSC, but this muscle tension is not displayed at all in AIC. This is because the subscapularis muscle does not have moment arm in the direction of abduction, but has moment arm in the direction of external rotation, and so the muscle is inhibited completely in AIC. The subscapularis muscle exhibits large model error, and thus muscle tension emerges in the unintended direction of external rotation. To keep the current joint angle against this motion, the deltoid(front) must exhibit large muscle tension, and this causes wasteful muscle tension by pulling at each other unnecessarily in MSC. Additionally, from 40 [sec], three deltoid muscles have even muscle tension because muscles with small moment arm to move in the intended direction are inhibited, movements other than abduction and adduction are permitted, and small muscle load sharing occurs, as discussed in the previous section. An example of a study in muscle load sharing is [8]. In this example, agonist muscles must be chosen ourselves, but we can inhibit antagonist muscles and share muscle load at the same time using the antagonistic decision part of this study.

B. Movement Using Scapula by AIC

The scapula is driven by seven muscles, #1–#7, of those in Fig. 9. The experimental motion is doing elevation, depression, upward rotation, and downward rotation continuously as shown in Fig. 12. The results of this experiment are indicated in Fig. 13. In AIC, the antagonist muscle, the Latissimus dorsi, is inhibited and this decreases the peak of muscle tension. However, Kengoro's scapula has only a small amount of muscle per freedom of scapula, so antagonistic muscles hardly emerge. Additionally, the workspace of joints is small, so the model error is small as well. Thus, although the maximum muscle tension decreased
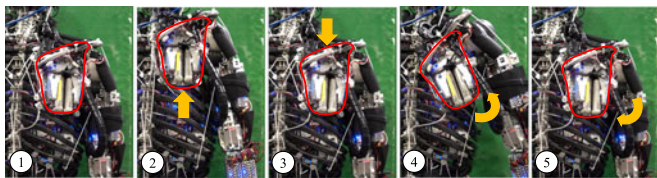
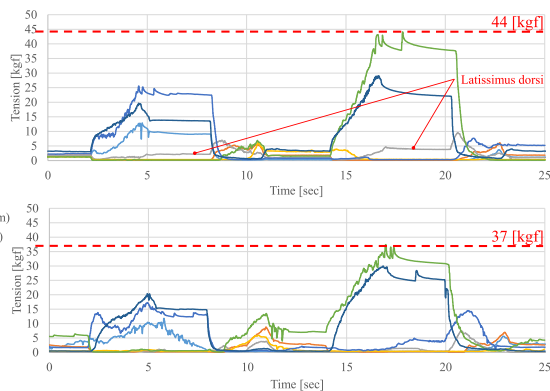Fig. 12.   Experimental motion of scapula.

Fig. 13.   Result of scapula motion experiment. Comparison of muscle tension between muscle stiffness control (upper graph) and antagonist inhibition control (lower graph).

from 44 [kgf] to 37 [kgf], AIC was not as effective as it was in movement using the shoulder.

C. Movement Using Scapula and Shoulder by AIC

We conducted wide range motion experiments of raising the arm upwards using the scapula and shoulder. In this movement, the scapula rotates upward by 60 [deg] when the abduction of the shoulder is by 120 [deg], and finally raises the arm to 180 [deg]. The experimental movement is raising the arm and putting them down continuously as shown in Fig. 14. The results of this experiment are indicated in Fig. 15. First, the maximum muscle tension is 55 [kgf] in MSC and is 45 [kgf] in AIC, showing that AIC can ease muscle tension. In MSC, the trapezius(upper), which shows maximum muscle tension, emerges beyond the tension limit of the tension measurement unit, leveling off the muscle tension, and is actually thought to be a higher value of about 60 to 70 [kgf]. Second, regarding the distribution of high tension muscles, in AIC, the infraspinatus muscle and subscapularis muscle, which do not have moment arm in the direction of abduction, are inhibited, but in MSC, the two muscles exhibit high tension against each other, as in the experiment on the shoulder motion. Additionally, in AIC, the trapezius(upper and bottom) is used to move the scapula, but in MSC, only the trapezius(upper) is used due to model error, and very high tension emerges. Finally, muscle tension increases like that of a human in AIC. In MSC, maximum muscle tension emerged when raising the arm upward completely, but in the case of a human, we need maximum torque and muscle tension when raising the arm to 90 [deg]. In AIC, model error is absorbed and only necessary muscle tension emerges, so muscle tension increases like that of a human.
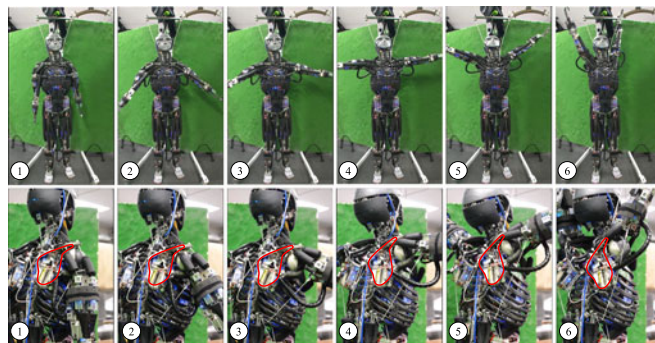

Fig. 14.   Experimental motion of raising arm by using scapula and shoulder. Front view (upper) and side view (lower).
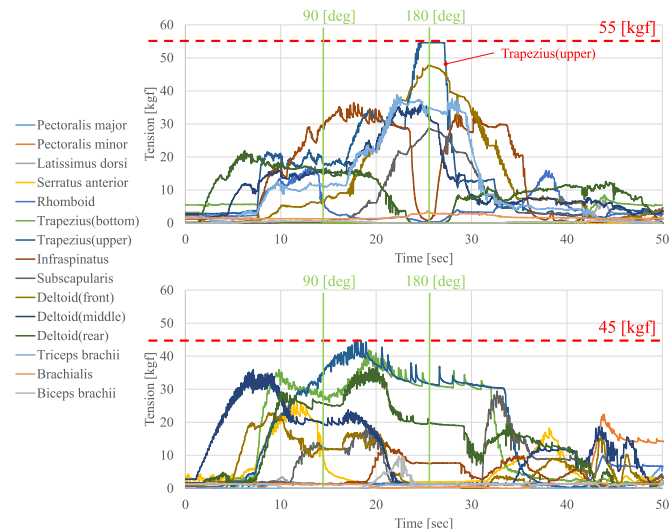

Fig. 15.   Result of raising arm motion experiment. Comparison of muscle tension between muscle stiffness control (upper graph) and antagonist inhibition control (lower graph).

D. Achievement of Long Time Dangling and Pull-Up

As presented so far, the simple control method of MSC, which follows target muscle length, is very dangerous because internal muscle tension due to model error increases as wide range motion becomes wider. Also, robots can only continue wide range motion for a short time due to the increase of temperature. As a final experiment of this study, we performed the dangling motion for a long time in order to verify the effectiveness of AIC. At the same time, we performed the pull-up motion, and considered future tasks based on the increase of muscle tension. As a reference, in Kengoro, links in the upper body cannot support the body by themselves like in ordinary robots, because the shoulder in a tendon-driven musculoskeletal humanoid is a ball joint and can dislocate. The motion results of the experiment are shown in Fig. 16. Kengoro holds onto a rod, lifts the rod while sending target length to raise the arms, and dangles. We did the pull-up motion three times, and made various poses while dangling for 14 minutes after that. As shown in upper graph of Fig. 17, except for the pull-up motion, the muscles did not increase in temperature, and we were able to show that robots can realize wide range motion safely for a long time using AIC.
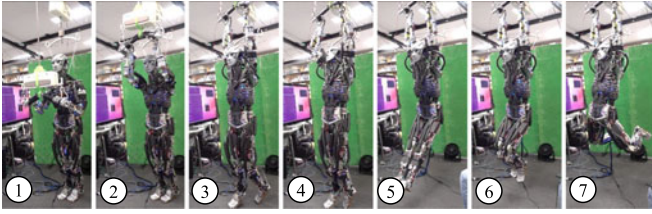
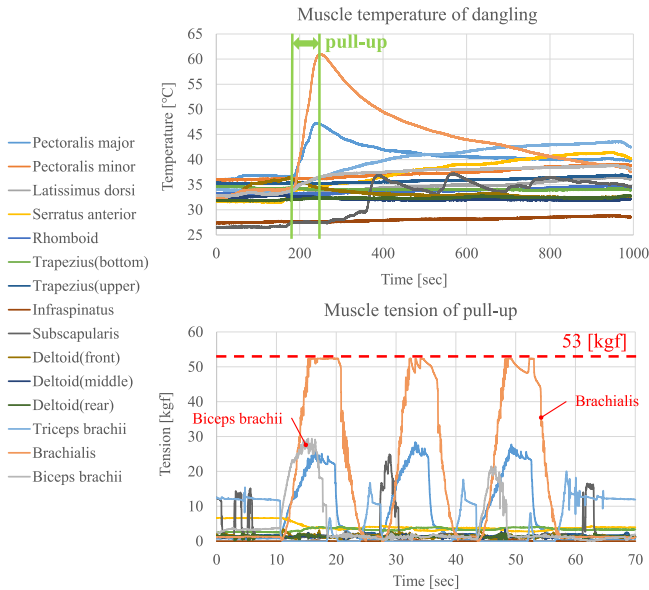Fig. 16.   Motion of pull-up (3–4) and dangling (5–7).

Fig. 17.   Muscle temperature of dangling (upper graph) and muscle tension of pull-up motion (lower graph).

Additionally, the muscle tension during a pull-up is shown in lower graph of Fig. 17. We were able to avoid high internal muscle tension by using AIC, and the subscapularis muscle, which normally has large model error, did not exhibit high tension at all. However, Kengoro could not move the elbow joint correctly during the pull-up motion. This is thought to be because the brachialis muscle had achieved maximum tension. To move the elbow joint correctly, Kengoro needs the cooperation of the brachialis muscle and biceps brachii muscle, and integration of muscle load sharing [8] with AIC.

VI. CONCLUSION

In this study, we explained the realization of wide range motion using antagonist inhibition control (AIC), which is based on reciprocal innervation in the human nervous system. By deciding between agonist or antagonist muscle from the muscle jacobian and inhibiting antagonist muscles, we can prevent inhibition of motion due to model error, fatal damage to the muscle and structure, and muscle slack without a perfect geometric model. Through the experiments of the shoulder and scapula, we showed that AIC can solve the problem that the wider the motion is, the more the internal muscle tension increases in the usual method of movement called Muscle Stiffness Control (MSC). We also showed that wide range motion such as pull-up and dangling, which is very dangerous due to the accumulating internal muscle tension, can be done safely for a long time by using AIC.

In future works, since wide range motion was achieved, we aim to do these motions more speedily and accurately through machine learning of model error. Because the tendon-driven musculoskeletal humanoid has a complex body based on a human, we believe that the meaning of this study lies in the acquisition of the self-body beyond achieving wide range motion.

REFERENCES

[1] M. Jäntsch, S. Wittmeier, K. Dalamagkidis, A. Panos, F. Volkart, and A. Knoll, "Anthrob—A printed anthropomimetic robot," in *Proc. 2013 IEEE-RAS Int. Conf. Humanoid Robots*, 2013, pp. 342–347.

[2] Y. Asano *et al.*, "Human mimetic musculoskeletal humanoid Kengoro toward real world physically interactive actions," in *Proc. 2016 IEEE-RAS Int. Conf. Humanoid Robots*, 2016, pp. 876–883.

[3] T. Shirai, J. Urata, Y. Nakanishi, K. Okada, and M. Inaba, "Whole body adapting behavior with muscle level stiffness control of tendon-driven multijoint robot," in *Proc. 2011 IEEE Int. Conf. Robot. Biomimetics*, 2011, pp. 2229–2234.

[4] S. C. Jacobsen, H. KO, E. K. Iversen, and C. C. Davis, "Control strategies for tendon-driven manipulators," *IEEE Control Syst. Mag.*, vol. 10, no. 2, pp. 23–28, Feb. 1990.

[5] V. Potkonjak, B. Svetozarevic, K. Jovanovic, and O. Holland, "The puller-follower control of compliant and noncompliant antagonistic tendon drives in robotic systems," in *Proc. Int. J. Adv. Robot. Syst.*, 2011, pp. 143–155.

[6] M. Jäntsch, C. Schmaler, S. Wittmeier, K. Dalamagkidis, and A. Knoll, "A scalable joint-space controller for musculoskeletal robots with spherical joints," in *Proc. 2011 IEEE Int. Conf. Robot. Biomimetics*, 2011, pp. 2211–2216.

[7] M. Kawamura, S. Ookubo, Y. Asano, T. Kozuki, K. Okada, and M. Inaba, "A joint-space controller based on redundant muscle tension for multiple DOF joints in musculoskeletal humanoids," in *Proc. 2016 IEEE-RAS Int. Conf. Humanoid Robots*, 2016, pp. 814–819.

[8] Y. Asano *et al.*, "Motion generation of redundant musculoskeletal humanoid based on robot-model error compensation by muscle load sharing and interactive control device," in *Proc. 2013 IEEE-RAS Int. Conf. Humanoid Robots*, 2013, pp. 336–341.

[9] S. Ookubo, Y. Asano, T. Kozuki, T. Shirai, K. Okada, and M. Inaba, "Learning nonlinear muscle-joint state mapping toward geometric model-free tendon driven musculoskeletal robots," in *Proc. 2015 IEEE-RAS Int. Conf. Humanoid Robots*, 2015, pp. 765–770.

[10] Y. Asano *et al.*, "A sensor-driver integrated muscle module with high-tension measurability and flexibility for tendon-driven robots," in *Proc. 2015 IEEE/RSJ Int. Conf. Intell. Robots Syst.*, 2015, pp. 5960–5965.